INTERNATIONAL JOURNAL OF QUANTUM CHEMISTRY, VOL. XII, 609–622

Diagrammatic Perturbation Theory: Potential Curves for the Ground State of the Carbon Monoxide Molecule

STEPHEN WILSON*
Institute for Space Studies, New York, New York 10025, U.S.A.

Abstracts

Diagrammatic many-body perturbation theory is used to calculate the potential energy function for the $X^1\Sigma^+$ state of the CO molecule near the equilibrium nuclear configuration. Spectroscopic constants are derived from a number of curves which are obtained from calculations taken through third order in the energy. By forming [2/1] Padé approximants to the constants we obtain: r_e = 1.125 Å (1.128 Å), B_e = 1.943 cm^{-1} (1.9312 cm^{-1}), α_e^B = 0.0156 cm^{-1} (0.0175 cm^{-1}), ω_e = 2247 cm^{-1} (2170 cm^{-1}), $\omega_e x_e$ = 12.16 cm^{-1} (13.29 cm^{-1}), where the experimental values are given in parenthesis.

La théorie des perturbations diagrammatique à N corps a été utilisée pour calculer l'énergie potentielle pour l'état $X^1\Sigma^+$ de la molécule CO près de l'équilibre. Des constantes spectroscopiques ont été calculées d'un nombre de courbes, obtenues de calculs des énergies jusqu'au troisième ordre. Les approximants de Padé de type [2/1] pour les constantes donnent: r_e = 1.125 Å (1.128 Å), B_e = 1.943 cm^{-1} (1.9312 cm^{-1}), α_e^B = 0.0156 cm^{-1} (0.0175 cm^{-1}), ω_e = 2247 cm^{-1} (2170 cm^{-1}), $\omega_e x_e$ = 12.16 cm^{-1} (13.29 cm^{-1}), où les valeurs expérimentales sont données entre parenthèses.

Diagrammatische Vielteilchenstörungstheorie ist benutzt worden, um die Potentialenergiefunktion für den Zustand $X^1\Sigma^+$ des CO-Moleküls in der Nähe der Gleichgewichtskonfiguration zu berechnen. Spektroskopische Konstanten sind von einer Reihe von Kurven hergeleitet worden, die von Energieberechnungen bis zur dritten Ordnung erhalten worden waren. Die erhaltenen [2/1]-Padé-Approximanten der Konstante sind: r_e = 1.125 Å (1.128 Å), B_e = 1.943 cm^{-1} (1.9312 cm^{-1}), α_e^B = 0.0156 cm^{-1} (0.0175 cm^{-1}), ω_e = 2247 cm^{-1} (2170 cm^{-1}), $\omega_e x_e$ = 12.16 cm^{-1} (13.29 cm^{-1}), wo die Experimentalwerte in Klammern gegeben sind.

Introduction

Studies of the carbon monoxide molecule [1] at its equilibrium nuclear configuration have shown that diagrammatic perturbation theory [2, 3], when taken through third order in the energy [4], can provide an accuracy which compares favorably with other theoretical methods. In this paper, we extend this study by reporting potential curves for the $X^1\Sigma^+$ state of CO for each of the energy quantities which may be derived from the third-order perturbation expansion. However, since the Hartree–Fock model is used to generate a reference spectrum and, as is well known, this model does not usually describe molecular dissociation correctly, we shall confine our attention to those configurations close to equilibrium.

* National Research Council Resident Research Associate, supported by the National Aeronautics and Space Administration. Present address: Science Research Council, Daresbury Laboratory, Daresbury, Warrington WA4 4AD, England.

Two different reference Hamiltonian operators are employed. From the two corresponding perturbation expansions, we construct [2/1] Padé approximants [5] and variational upper bounds [4, 6–9] to the energy in addition to the usual truncated Taylor expansion. In this paper we compare the potential curves corresponding to each of these quantities and the spectroscopic constants, r_e, B_e, α_e^B, ω_e, $\omega_e x_e$, which may be derived from them.

The calculations are performed within the albebraic approximation [4]. The one-electron state functions are parameterized by expansion in a finite set of basis functions. This is necessary in order to apply the diagrammatic perturbation expansion to molecules other than those containing hydrogen atoms, which may be treated as an additional perturbation. The carbon monoxide molecule may be regarded as a prototype for such systems.

A study of the neon atom [4] has shown that the diagrammatic perturbation expansion, when taken through third order in the energy, provides an accuracy which is comparable with that afforded by the method of configuration interaction when the same basis set is employed. The relation between the diagrammatic many-body perturbation expansion and the method of configuration interaction has been explored previously [4].

In the following section, we give a brief outline of the diagrammatic perturbative expansion. More detailed discussions may be found elsewhere [2–4]. In the third section the resulting potential energy curves are given. Spectroscopic constants are presented in the fourth section. In the final section results are discussed.

Diagrammatic Perturbation Theory

The diagrammatic perturbation expansion, when taken through third order in the energy, not only provides an attractive pictorial representation of electron correlation effects but also forms the basis of a noniterative and computationally efficient algorithm [10] for electronic structure calculations to an accuracy well beyond that afforded by the Hartree–Fock model [4, 11, 12].

The correlation energy is given by the diagrammatic expansion

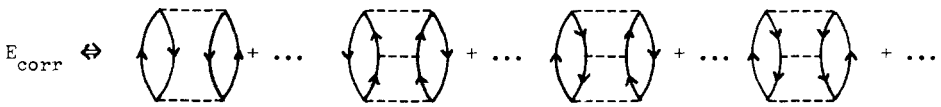

where only the parent Goldstone diagram of each set which are related by electron exchange is given. The first diagram is associated with second-order effects; the remaining diagrams are of third order. The analytic expressions corresponding to these diagrams are easily written down [4].

In this work, we shall denote a component of the correlation energy by E_b^a, where a is the number of bodies involved and b the order of perturbation. E_b denotes the total bth order energy but E^a will denote the total a-body energy

through third order. $E(c)$ will be used to denote the total energy through cth order.

Two different reference Hamiltonian operators are employed in this study: the Hartree–Fock *model* Hamiltonian and the *shifted* Hamiltonian [4]. The latter will be distinguished by placing a bar on the corresponding energy quantities.

From the third-order expansion for the energy we can construct the Padé approximant

$$E[2/1] = E_0 + E_1 + E_2/(1 - E_3/E_2) \tag{2}$$

This approximant has certain desirable invariance properties which are not shared by the Taylor expansion [5]. It is invariant to change of scale and shift of origin in the reference spectrum.

By substituting the first-order wave function

$$\Phi_0 + \gamma\Phi_1 \tag{3}$$

in the Rayleigh quotient, we obtain the upper bound [6–9]

$$E_{\text{var}}(\gamma) = E_0 + E_1 + ((2\gamma - \gamma^2)E_2 + \gamma^2 E_3)/(1 + \gamma^2 S) \tag{4}$$

where γ is a parameter whose optimal value may be determined by invoking the variation theorem and $S = \langle\Phi_1|\Phi_1\rangle$.

Potential Energy Functions

The basis set of Slater exponential functions used to parameterize the one-electron state functions in the present study is given in Table I. It is based on the

TABLE I. Basis set of Slater exponential functions.[a]

C :	1s (5.3767, 8.982); 2s (2.0131, 5.6319, 1.3089); $2p_\sigma$ (1.8076, 2.2398, 0.9554, 6.3438); $3d_\sigma$(2.65); $4f_\sigma$(2.06); $2p_\pi$(1.4209, 2.5873, 0.9554, 5.3438); $3d_\pi$(2.207); $4f_\pi$(2.9); $3d_\delta$(2.207); $4f_\delta$(2.9).
O :	1s(7.6063, 13.224); 2s(3.11196,6.3783,1.80848); $2p_\sigma$(1.796, 3.3379,1.1536,7.907); $3d_\sigma$(2.1144); $4f_\sigma$(2.5); $2p_\pi$(1.8171, 3.4379,1.1536,7.907); $3d_\pi$(2.2297); $4f_\pi$(2.482); $3d_\delta$(2.2297); $4f_\delta$(2.482).

[a] Orbital exponents are given in parenthesis.

set given by McLean and Yoshimine [13]. It consists of 54 functions: 22 of σ-symmetry, 24 of π-symmetry, and 8 of δ-symmetry. Calculations were performed at twelve nuclear separations in the range 1.8 to 3.0 bohrs using this basis set.

In Tables II and III we present the components of the calculated correlation energy as a function of the nuclear separation r. The variation of the second-order and third-order components is shown in Table II, while in Table III we show the

TABLE II. Variation of second- and third-order energies with nuclear separation.[a]

R	E_2	$\bar{E}_2$	E_3	$\bar{E}_3$
1.8	-0.3828	-0.4533	-0.0070	+0.0750
1.9	-0.3900	-0.4654	-0.0047	+0.0853
2.0	-0.3978	-0.4794	-0.0019	+0.0991
2.05	-0.4019	-0.4872	-0.0003	+0.1075
2.1	-0.4061	-0.4953	+0.0015	+0.1169
2.132	-0.4088	-0.5006	+0.0028	+0.1233
2.15	-0.4104	-0.5037	+0.0035	+0.1270
2.2	-0.4148	-0.5123	+0.0056	+0.1380
2.3	-0.4240	-0.5302	+0.0104	+0.1624
2.4	-0.4335	-0.5485	+0.0159	+0.1894
2.5	-0.4433	-0.5662	+0.0222	+0.2167
3.0	-0.4853	-0.6366	+0.0569	+0.3396

[a] Atomic units are used throughout.

variation of two-body, three-body, and four-body components of the correlation energy through third order. In both of these tables results are presented for the two reference Hamiltonian operators discussed above. The variations of the components of the correlation energy with r are sketched in Figure 1 for the perturbation expansion corresponding to the *model* reference Hamiltonian.

In Table IV the calculated potential energy functions for the ground state of the carbon monoxide molecule are displayed. Rigorous upper bounds to these curves are presented in Table V. Values of the variationally optimized parameter γ of Eq. (4) are also included in Table V. The [2/1] Padé approximant and upper bound to the energy obtained from the perturbation expansion generated by the Hartree–Fock model Hamiltonian are illustrated in Figure 2, together with the matrix Hartree–Fock potential energy curve.

Spectroscopic Constants

The solution of the electronic Schrödinger equation yields the potential energy function in tabular form. It is necessary to interpolate between these calculated values in order to determine spectroscopic constants. Power series expansions

TABLE III. Variation of two-, three- and four-body components of the correlation energy with nuclear separation.[a]

R	E^2	E^3	E^4	$\bar{E}^2$	$\bar{E}^3$	$\bar{E}^4$
1.8	-0.4510	+0.0583	+0.0029	-0.4729	+0.0905	+0.0040
1.9	-0.4611	+0.0632	+0.0031	-0.4850	+0.1004	+0.0044
2.0	-0.4718	+0.0686	+0.0034	-0.4981	+0.1127	+0.0051
2.05	-0.4773	+0.0715	+0.0036	-0.5050	+0.1199	+0.0054
2.1	-0.4830	+0.0746	+0.0038	-0.5121	+0.1277	+0.0059
2.132	-0.4867	+0.0766	+0.0040	-0.5167	+0.1330	+0.0063
2.15	-0.4888	+0.0778	+0.0041	-0.5193	+0.1362	+0.0065
2.2	-0.4947	+0.0811	+0.0044	-0.5267	+0.1453	+0.0071
2.3	-0.5069	+0.0883	+0.0050	-0.5419	+0.1655	+0.0086
2.4	-0.5197	+0.0963	+0.0058	-0.5577	+0.1882	+0.0104
2.5	-0.5330	+0.1054	+0.0066	-0.5742	+0.2125	+0.0123
3.0	-0.5964	+0.1599	+0.0082	-0.6573	+0.3435	+0.0167

[a] Atomic units are used throughout.

TABLE IV. Potential energy curves for the $X^1\Sigma^+$ state of the carbon monoxide molecule.[a]

R	E_{ref}	E(3)	$\bar{E}(3)$	$E[2/1]$	$\bar{E}[2/1]$
1.8	-112.70248	-113.0923	-113.0808	-113.0924	-113.0915
1.9	-112.75831	-113.1531	-113.1385	-113.1532	-113.1517
2.0	-112.78486	-113.1846	-113.1652	-113.1846	-113.1822
2.05	-112.78990	-113.1921	-113.1696	-113.1921	-113.1890
2.1	-112.79058	-113.1951	-113.1690	-113.1951	-113.1913
2.132	-112.78907	-113.1951	-113.1664	-113.1952	-113.1908
2.15	-112.78762	-113.1945	-113.1643	-113.1946	-113.1899
2.2	-112.78163	-113.1908	-113.1560	-113.1908	-113.1852
2.3	-112.76255	-113.1761	-113.1304	-113.1764	-113.1685
2.4	-112.73668	-113.1543	-113.0958	-113.1548	-113.1444
2.5	-112.70647	-113.1276	-113.0559	-113.1286	-113.1159
3.0	-112.53920	-112.9675	-112.8362	-112.9735	-112.9544

[a] Atomic units are used throughout.

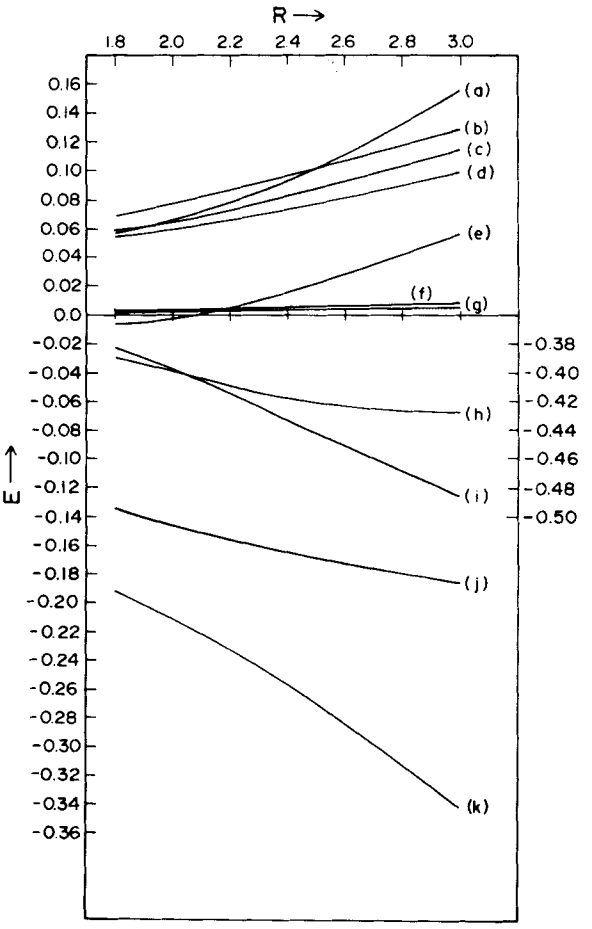

Figure 1. Variation of the components of the correlation energy resulting from the *model* perturbation expansion with changing internuclear separation. The components are: (a) E_3^3 (hole–particle); (b) E_3 (particle–particle); (c) E_3 (hole–hole); (d) E_3^2 (hole–hole); (e) E_3; (f) E_3^4 (hole–hole); (g) E_3^3 (hole–hole); (h) E_2+E_3; (i) E_2; (j) E_3 (hole–particle); (k) E_3^2 (hole–particle). All curves refer to the left-hand scale except curves (h) and (i) which refer to the right-hand scale.

provide a reasonably general means of doing this for nuclear separations close to equilibrium.

In the present work we fit the calculated energy values to the expansion [14]

$$V(\rho) = A_0\left[1 + \sum_{i=1} a_i \rho^i\right] \tag{5}$$

where

$$\rho = (r - r_e)/r_e \tag{6}$$

TABLE V. Upper bounds to the potential energy curve for the $X^1\Sigma^+$ state of the carbon monoxide molecule.[a]

R	$E_{var}(\gamma=1)$	$\bar{E}_{var}(\gamma=1)$	$E_{var}(\gamma_{opt})$	$\bar{E}_{var}(\gamma_{opt})$	γ_{opt}	$\bar{\gamma}_{opt}$
1.8	-113.0629	-113.0380	-113.0641	-113.0605	0.9447	0.7898
1.9	-113.1214	-113.0918	-113.1230	-113.1186	0.9351	0.7743
2.0	-113.1504	-113.1142	-113.1526	-113.1470	0.9245	0.7554
2.05	-113.1565	-113.1162	-113.1591	-113.1528	0.9188	0.7448
2.1	-113.1582	-113.1132	-113.1613	-113.1540	0.9129	0.7337
2.132	-113.1573	-113.1091	-113.1607	-113.1528	0.9089	0.7265
2.15	-113.1561	-113.1060	-113.1597	-113.1515	0.9067	0.7223
2.2	-113.1509	-113.0952	-113.1551	-113.1457	0.9003	0.7107
2.3	-113.1330	-113.0647	-113.1385	-113.1268	0.8868	0.6870
2.4	-113.1078	-113.0256	-113.1149	-113.1007	0.8725	0.6637
2.5	-113.0775	-112.9817	-113.0867	-113.0703	0.8577	0.6426
3.0	-112.9000	-112.7511	-112.9228	-112.9006	0.7904	0.5677

[a] Atomic units are used throughout.

The radius of convergence of such an expansion is $0<r<2r_e$, where r_e is the equilibrium nuclear separation. An eighth-order polynomial was used to interpolate the reference energies and a fourth-order polynomial to interpolate the correlation energy corrections. The accuracy of this technique has been discussed previously [15]. In the fitting procedure we included all of the calculated points except that at $r = 2.132$ bohrs.

The rotation constant B_e calculated from the matrix Hartree–Fock reference potential energy curve, 2.023 cm^{-1}, agrees well with the value given by Huo [16], 2.027 cm^{-1}. Similar good agreement was found for the calculated fundamental frequency of vibration; namely, 2438 cm^{-1} compared with Huo's value of 2431 cm^{-1}.

In Tables VI–X calculated spectroscopic constants are presented. In Table XI the change in the spectroscopic constants with increasing order of the energy are demonstrated. Thus X_1 denotes a quantity calculated from the matrix Hartree–Fock reference potential function X_2 a quantity derived from the second-order curve, and X_3 from the third-order curve. The values given in Table XI, correspond to the *model* perturbation expansion which has been found to be the more rapidly convergent for the energy.

Discussion

As was the case in our studies of other systems [4, 11, 15], the *model* perturbation expansion appears to be the more rapidly convergent of the two

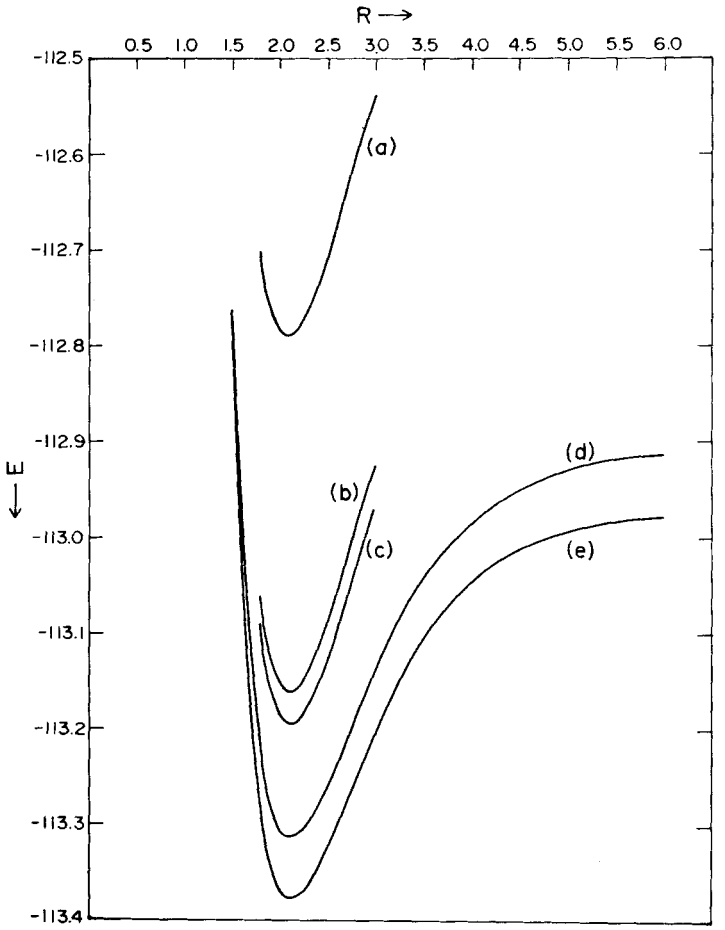

Figure 2. Potential curves for the $X^1\Sigma^+$ state of the carbon monoxide molecule. Curve a is the Hartree–Fock potential energy function. Curve b corresponds to the E_{var} (γ_{opt}) energy values while curve c results from the Padé approximant E [2/1]. Curves d and e are derived from the experimental data. The latter is the Morse function determined by the experimentally determined values of r_e, D_e, and ω_e, while the former includes an empirical correction for the relativistic energy.

expansions considered in this work. In Figure 3, we show the differences between the energies derived from the two perturbation expansions as a function of nuclear separation. The use of the [2/1] Padé approximants and the optimized upper bounds represent considerable improvements on the values of $E(3)$ and $\bar{E}(3)$.

A more detailed analysis of the correlation energy corresponding to the *model* perturbation expansion is presented in Figure 1. It shows several interesting features which have been confirmed in studies of other systems [15]. $E_3^4(hh)$ is very small and yet represents the entire four-body component. $E_3^3(hh)$ is negligible and thus $E_3^3(hp)$ represents the only significant three-body effect and by

TABLE VI. Comparison of calculated equilibrium nuclear separations.[a]

Reference $\mathcal{H}_0$	$\mathcal{H}_{\text{model}}$	$\mathcal{H}_{\text{shifted}}$	Δ[b]
E(2)	1.136	1.182	0.046
E(3)	1.120	1.095	0.025
E[2/1]	1.120	1.114	0.006
$E_{\text{var}}(\gamma=1)$	1.109	1.082	0.027
$E_{\text{var}}(\gamma_{\text{opt}})$	1.113	1.106	0.007

[a] Angstrom units are used throughout.
[b] $\Delta = |r_{e,\text{model}} - r_{e,\text{shifted}}|$.

TABLE VII. Comparison of calculated rotation constants, B_3.[a]

Reference $\mathcal{H}_0$	$\mathcal{H}_{\text{model}}$	$\mathcal{H}_{\text{shifted}}$	Δ[b]
E(2)	1.906	1.759	0.147
E(3)	1.961	2.051	0.090
E[2/1]	1.961	1.983	0.022
$E_{\text{var}}(\gamma=1)$	1.998	2.101	0.103
$E_{\text{var}}(\gamma_{\text{opt}})$	1.987	2.010	0.023

[a] cm^{-1} are used throughout.
[b] $\Delta = |B_{e,\text{model}} - B_{e,\text{shifted}}|$.

TABLE VIII. Comparison of calculated vibration–rotation interaction constants, αB.[a]

Reference $\mathcal{H}_0$	$\mathcal{H}_{\text{model}}$	$\mathcal{H}_{\text{shifted}}$	Δ[b]
E(2)	0.0163	0.0287	0.0124
E(3)	0.0147	0.0099	0.0048
E[2/1]	0.0151	0.0140	0.0011
$E_{\text{var}}(\gamma=1)$	0.0139	0.0100	0.0039
$E_{\text{var}}(\gamma_{\text{opt}})$	0.0147	0.0139	0.0008

[a] cm^{-1} are used throughout.
[b] $\Delta = |\alpha^B_{\text{model}} - \alpha^B_{\text{shifted}}|$.

TABLE IX. Comparison of calculated fundamental frequencies of vibration, ω_e.[a]

Reference $\mathcal{H}_0$	$\mathcal{H}_{model}$	$\mathcal{H}_{shifted}$	Δ[b]
E(2)	2133	1771	362
E(3)	2316	2676	360
E[2/1]	2308	2398	90
$E_{var}(\gamma=1)$	2416	2797	381
$E_{var}(\gamma_{opt})$	2370	2457	87

[a] cm^{-1} are used throughout.
[b] $\Delta = |\omega_{e,model} - \omega_{e,shifted}|$.

TABLE X. Comparison of calculated anharmonicity constants, $\omega_e x_e$.[a]

Reference $\mathcal{H}_0$	$\mathcal{H}_{model}$	$\mathcal{H}_{shifted}$	Δ[b]
E(2)	13.44	7.29	6.15
E(3)	10.41	7.63	2.78
E[2/1]	10.92	10.88	0.04
$E_{var}(\gamma=1)$	9.78	8.12	1.66
$E_{var}(\gamma_{opt})$	10.74	10.92	0.18

[a] cm^{-1} are used throughout.
[b] $\Delta = |(\omega_e x_e)_{model} - (\omega_e x_e)_{shifted}|$.

far the most important many-body component. Thus $E^3 \simeq E_3^3(hp)$ and $E^3(hh) \simeq E_3^2(hh)$. We also note that $E^3(hh) \simeq E_3(pp) \simeq E_3^3(hp)$. All of the components discussed so far are positive; E_2 and $E_3^2(hp)$ are negative. There is a large cancellation among the components of the third-order energy and the total is relatively small.

The potential curves corresponding to the [2/1] Padé approximant and the optimized upper bound for the *model* perturbation expansion are compared with other relevant curves in Figure 2. Curve d includes an empirical correction for the relativistic energy. It is assumed that the relativistic energy is independent of the nuclear geometry and equal to the sum of the relativistic energy of the carbon and oxygen atoms as given by Veillard and Clement [17]. (The small Lamb corrections are ignored.)

It is clear from Tables VI–X that the use of the potential energy curves corresponding to the [2/1] Padé approximants and the optimized upper bounds

TABLE XI. Spectroscopic constants corresponding to first-, second- and third-order potential curves derived from the perturbation expansion in which the Hartree–Fock operator is used as a reference Hamiltonian.

Property	r_e	B_e	α_e^B	ω_e	$\omega_e x_e$
X_1	1.102	2.023	0.0149	2438	11.24
ΔX_2	+0.034	−0.117	+0.0014	−305	+2.20
X_2	1.136	1.906	0.0163	2133	13.44
ΔX_3	−0.016	+0.055	−0.0016	+183	−3.03
X_3	1.120	1.961	0.0147	2316	10.41
$\Delta X_3/\Delta X_2$	−0.47	−0.47	−1.14	−0.60	−1.38
$X[2/1]$	1.125	1.943	0.0156	2247	12.16

X_i denotes the property X calculated from the ith order potential curve; thus X_1 is a property calculated from the matrix Hartree–Fock potential curve. ΔX_i denotes the change in the property X on going from the $(i-1)$th order potential curve to the ith order potential curve. r_e is in Angstroms; all other quantities are in cm^{-1}.

leads to closer agreement between spectroscopic constants derived from the *model* and the *shifted* perturbation expansions than does the use of the other energy values. Spectroscopic constants derived from the *model* expansion change less than those derived from the *shifted* expansion on going from second order to third order. This suggests that the constants derived from the *model* expansion converge more rapidly than those derived from the *shifted* series. The convergence of the spectroscopic constants with order of perturbation for the *model* expansion is shown in Table XII. $\Delta X_3/\Delta X_2$ may be regarded as a qualitative measure of convergence. Note that the value of this ratio for the spectroscopic constants is considerably larger than E_3/E_2, which at $r = 2.132$ bohrs, takes the value -0.007. We note also that the ratio is negative for the cases considered here. Based on experience in calculations of the energy [1, 4, 11, 12], we make the conjecture that the Padé approximant

$$X[2/1] = X_1 + \Delta X_2/(1 - \Delta X_3/\Delta X_2) \tag{7}$$

will form a useful representation of the property X. This approximant has been constructed for the properties considered in this work and is given in the final row of Table XII.

The calculated spectroscopic constants are compared with the experimental results in Table XI. The Padé approximants X [2/1] are uniformly closer to experiment than the simple third-order results are. The closeness of some of the second-order results to experiment is probably fortuitous. The calculated con-

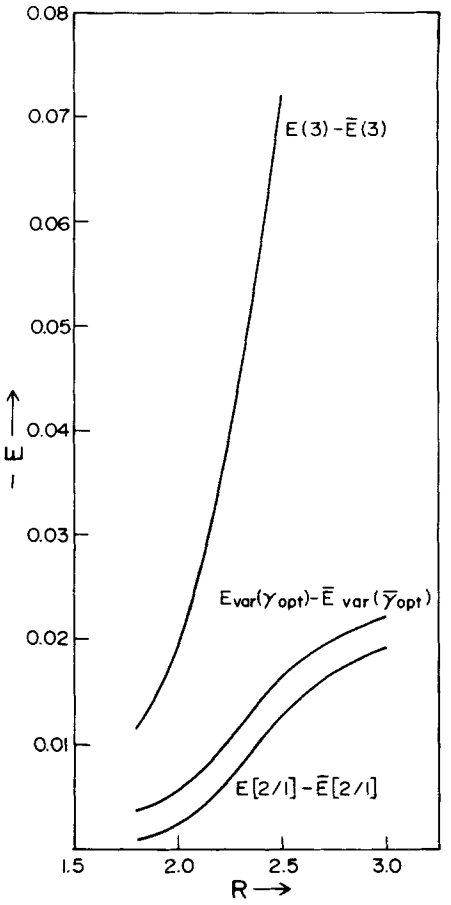

Figure 3. Differences between the energy values corresponding to the *model* and *shifted* perturbation expansions as a function of nuclear separation.

stants are uniformly biased towards the Hartree–Fock values. Thus, for example, the calculated value of the equilibrium internuclear distance r_e [2/1] differs from the experimental value by 0.003 Å and is biased towards the Hartree-Fock value, which differs from the experimental value by 0.026 Å. 89% of the difference between the Hartree–Fock value of r_e and the experimental r_e is accounted for by the present calculation.

Many *ab initio* studies of the ground state of the carbon monoxide molecule have been reported previously [18]. Siu and Davidson [19] obtained a total energy of −113.1456 hartree at a nuclear separation of 2.132 bohrs using the method of configuration interaction. This should be compared with the values given in Tables IV and V. A detailed comparison of third-order diagrammatic perturbation theory and the method of configuration interaction for the ground state of the CO molecule at its equilibrium geometry has been given [1]. Hall et al. [20] have

TABLE XII. Comparison of calculated spectroscopic constants with experimentally determined values.*

Potential function	r_e(Å)	B_e(cm^{-1})	α_e^B(cm^{-1})	ω_e(cm^{-1})	$\omega_e\chi_e$(cm^{-1})
Experiment	1.128	1.9312	0.0175	2170	13.29
E_{ref}	1.102	2.023	0.0149	2438	11.24
	(2.3%)	(4.8%)	(14.8%)	(12.4%)	(15.4%)
E(2)	1.136	1.906	0.0163	2133	13.44
	(0.7%)	(1.3%)	(6.9%)	(1.7%)	(1.1%)
E(3)	1.120	1.961	0.0147	2316	10.41
	(0.7%)	(1.5%)	(16%)	(6.7%)	(21.7%)
E[2/1]	1.120	1.961	0.0151	2308	10.92
	(0.7%)	(1.5%)	(13.7%)	(6.4%)	(17.9%)
$E_{var}(\gamma_{opt})$	1.113	1.987	0.0147	2370	10.74
	(1.3%)	(2.9%)	(16%)	(9.2%)	(19.2%)
X[2/1]	1.125	1.943	0.0156	2247	12.16
	(0.3%)	(0.6%)	(10.9%)	(3.5%)	(8.5%)

* The percentage difference between the theoretical and experimental values is given in parenthesis.

used configuration interaction to obtain theoretical values of the equilibrium bond distance and the fundamental frequency of vibration. For the former they obtained $r_e = 1.138$ Å while for the latter they reported $\omega_e = 2000$ cm^{-1}. These values differ from experiment by 0.9 and 7.8%, respectively.

Finally, we remark that the present approach to the accurate calculation of potential functions is computationally tractable. It forms the basis of an efficient and non-iterative algorithm [10].

Bibliography

[1] R. J. Bartlett, S. Wilson, and D. M. Silver, Int. J. Quant. Chem., to appear.
[2] N. H. March, W. H. Young, and S. Sampanthar, *The Many-Body Problem in Quantum Mechanics* (Cambridge Univ. Press, England, 1967).
[3] H. P. Kelly, Advan. Chem. Phys. **14**, 129 (1969).
[4] S. Wilson and D. M. Silver, Phys. Rev. **A14**, 1949 (1976).
[5] S. Wilson, D. M. Silver, and R. A. Farrell, Proc. R. Soc. (London) **356**, 363 (1977).
[6] W. H. Young and N. H. March, Phys. Rev. **109**, 1854 (1958).
[7] A. Dalgarno and A. L. Stewart, Proc. Phys. Soc. (London) **77**, 467 (1961).
[8] O. Goscinski and E. Brandas, Chem. Phys. Lett. **2**, 299 (1968).
[9] R. J. Bartlett and D. M. Silver, Int. J. Quant. Chem. **9**, 183 (1975).
[10] D. M. Silver, Comp. Phys. Commun. (in press). S. Wilson, Comp. Phys. Commun. (in press).

[11] S. Wilson and D. M. Silver, J. Chem. Phys. **66**, 5400 (1977).
[12] S. Wilson, D. M. Silver, and R. J. Bartlett, Molec. Phys. **33**, 1177 (1977).
[13] A. D. McLean and M. Yoshimine, IBM J. Res. Develop. Suppl. (1967).
[14] J. L. Dunham, Phys. Rev. **41**, 721 (1932).
[15] S. Wilson, Molec. Phys., to appear.
[16] W. M. Huo, J. Chem. Phys. **43**, 624 (1965).
[17] A. Veillard and E. Clementi, J. Chem. Phys. **49**, 2419 (1968).
[18] W. G. Richards, T. E. H. Walker, and R. K. Hinkley, *Bibliography of ab initio Molecular Wave Functions* (Clarendon Press, Oxford, 1971); W. G. Richards, E. H. Walker, L. Farnell, and P. R. Scott, *Supplement,* 1974.
[19] A. K. Q. Siu and E. R. Davidson, Int. J. Quant. Chem. **4**, 223 (1970).
[20] J. A. Hall, J. Schamps, J. M. Robbe, and H. Lefebvre-Brion, J. Chem. Phys. **59**, 3271 (1973).
[21] I. M. Mills, *Specialist Periodical Reports—Theoretical Chemistry*, vol. 1, 1974.

Received April 15, 1977
Revised May 13, 1977
Accepted for publication May 17, 1977